American Mineralogist, Volume 78, pages 1217–1229, 1993

Smectite-group minerals in deep-sea sediments: Monomineralic solid-solutions or multiphase mixtures?

Hojatollah Vali, Robert F. Martin
Department of Earth and Planetary Sciences, McGill University, 3450 University Street, Montreal, Quebec H3A 2A7, Canada
Georgios Amarantidis,* Giulio Morteani
Lehrstuhl für Angewandte Mineralogie und Geochemie, Technische Universität München, Lichtenbergstraße 4, D-8046 Garching, Germany

Abstract

Results of XRD, TEM, and chemical analyses are combined to characterize the true chemistry and structural formula of the smectite-group minerals present in selected samples of deep-sea sediments from the north-central Pacific and Angola, Lau, and North Fiji Basins. In most cases, the abundant Fe and K in the <0.2-μm fraction is associated with accessory minerals such as mica, phillipsite, and iron oxides. Bulk analytical data obtained from the <0.2-μm fraction, corrected for the presence of these minerals, reveal a structural formula very close to that of ideal montmorillonite. The extensive chemical variability among members of the clay-mineral group usually is attributed to the occurrence of solid solution. The variability in smectite-group minerals also could be due to (1) the occurrence of mixed-layer structures, (2) the presence of compositionally distinct domains in the structure, or (3) a mixture of two or more distinct phases. A clear distinction between a monomineralic solid-solution phase and a mixture of coexisting end-members based on chemical composition or even conventional XRD and HRTEM techniques is of crucial importance. The data presented in the literature concerning the nature of the smectite-group phase and related I/S mixed layers do not necessarily reflect the true nature of the individual clay-mineral phases. The application of the term "smectite" to a material characterized by a structural formula should be avoided.

Introduction

A valid structural formula (Köster, 1977; Newman and Brown, 1987), derived from chemical data, provides one of the most common bases of classification of clay-mineral phases. However, in most cases, sample heterogeneity and the presence of contamination, even in the finest clay-size fractions (<0.05 μm), do not permit the determination of the actual chemical composition of individual clay-mineral phases. According to Warren and Ransom (1992), compositional variations in populations of clay minerals reported in the literature commonly are the result of sample contamination and analytical uncertainties. As an example of a submicroscopic contaminant, consider the abundant single-domain magnetic particles in clay-size fractions of deep-sea sediments from the Pacific and south Atlantic oceans (Vali et al., 1987; Vali and Kirschvink, 1989). In previous studies of such material (e.g., Hein et al., 1979; Karpoff, 1984), the possibility of a contribution by such an iron oxide contaminant was ignored in the determination of the chemical composition of the smectite-group minerals. Indeed, the extensive chemical variability among minerals of the smectite group usually is attributed to the occurrence of solid solution (Velde, 1985; Velde and Brusewitz, 1986; Velde and Meunier, 1987; Newman and Brown, 1987). In this study, we attempt to characterize the true chemical compositions and structural formulas of the smectite-group minerals present in selected samples of deep-sea sediments. The likelihood of monomineralic solid solutions is evaluated by comparing results obtained by transmission electron microscopy with bulk chemical data for the <0.2-μm fraction.

Terminology

For purposes of this paper, the word "smectites" is avoided in favor of "smectite-group minerals." Montmorillonite, beidellite, and nontronite are used as end-members of the dioctahedral smectite group of minerals. Chemical variation within mineral species is expressed here by terms like Fe-rich montmorillonite or Al-poor nontronite. We deliberately avoid using terms like "Fe-smectite" and "Fe-montmorillonite," which contravene a basic rule of nomenclature of minerals, as promulgated by the Committee of New Minerals and Mineral Names of International Mineralogical Association (Nickel and Mandarino, 1987).

* VAW Flußspat Chemie GmbH, Postfach 1168, D-8470 Stulln/Nabburg, Germany.

0003–004X/93/1112–1217$02.00

Table 1. Location of deep-sea sediments and proportion of carbonate fraction

Core	Coordinates	Water depth (m)	Depth of drill core (m)	$CaCO_3$ (vol%)
North-central Pacific (SO-25)				
133-KL	12°25′N, 150°13′W	5426	4.60–4.65	0.9
177-KL	9°19′N, 146°6′W	5314	3.10–3.15	1.0
184-KL	9°17′N, 146°9′W	5334	8.00–8.05	0.6
315-KL	7°57′N, 143°33′W	5200	5.20–5.25	0.6
383-KL	8°5′N, 143°33′W	5211	2.40–2.45	2.2
Angola Basin (Leg 73)				
522-10	26°06′S, 5°07′W	4441	37.2–41.2	2.1
522-14	26°06′S, 5°07′W	4441	50.7–55.1	16.2
522-37	26°06′S, 5°07′W	4441	139.7–147.7	88.3
523-26	28°33′S, 2°15′W	4562	92.8–98.8	90.2
523-37	28°33′S, 2°15′W	4562	130.8–135.2	52.5
523-44	28°33′S, 2°15′W	4562	159.7–166.7	85.4
North Fiji Basin (SO-35)				
182-KL	14°30′S, 177°05′E	3010	2.75–2.80	72.2
182-KL	14°30′S, 177°05′E	3010	5.10–5.14	74.1
182-KL	14°30′S, 177°05′E	3010	12.45–12.50	74.8
184-KL	14°25′S, 177°06′E	2865	6.02–6.07	80.1
243-KL	14°37′S, 177°22′E	2415	10.03–10.08	78.7
254-KL	15°15′S, 177°12′E	2985	1.60–1.65	67.3
Lau Basin (SO-35)				
110-KL	22°15′S, 177°20′W	2970	6.25–6.30	66.0
119-KL	22°00′S, 177°17′W	2365	1.00–1.05	51.2
119-KL	22°00′S, 177°17′W	2365	1.55–1.60	58.2
119-KL	22°00′S, 177°17′W	2365	6.30–6.35	50.3
119-KL	22°00′S, 177°17′W	2365	9.86–9.91	60.2
120-KL	22°00′S, 177°07′W	2625	4.05–4.10	50.5

Table 2. Distribution of size fractions

Core/ site	Depth (m)	1	2	3	4	5	6	7
North-central Pacific (SO-25)								
133-KL	4.60–4.65	26.4	16.8	21.7	20.7	10.0	1.6	2.8
177-KL	3.10–3.15	29.5	21.0	21.4	21.7	5.9	0.3	0.1
184-KL	8.00–8.05	27.8	19.6	25.5	20.9	5.5	0.7	0.1
315-KL	5.20–5.25	24.1	19.6	18.4	24.6	10.9	1.3	1.1
383-KL	2.40–2.45	27.6	22.7	22.6	21.3	5.4	0.4	0.0
Angola Basin (Leg 73)								
522-10	37.2–41.2	44.9	16.5	19.5	13.7	4.6	0.8	0.0
522-14	50.7–55.1	33.6	17.0	19.9	17.4	11.5	0.7	0.0
522-37	139.7–147.7	50.0	14.1	16.5	12.5	6.2	0.6	0.0
523-26	92.8–98.8	48.9	11.6	14.8	16.6	7.5	0.6	0.0
523-37	130.8–135.2	53.8	11.5	13.4	12.3	8.0	1.1	0.0
523-44	159.7–166.7	54.5	13.3	12.0	12.8	7.4	0.0	0.0
North Fiji Basin (SO-35)								
182-KL	2.75–2.80	26.6	10.2	12.4	23.5	17.3	7.1	2.8
182-KL	5.10–5.14	20.5	18.3	16.0	25.7	15.7	2.7	1.1
182-KL	12.45–12.50	17.5	12.6	28.8	23.0	12.2	5.6	0.3
184-KL	6.02–6.07	13.1	24.3	27.6	19.6	11.8	3.1	0.5
243-KL	10.03–10.08	54.3	8.0	10.8	7.1	15.2	3.2	1.3
254-KL	1.60–1.65	30.5	15.2	2.8	22.0	19.2	10.1	0.3
Lau Basin (SO-35)								
110-KL	6.25–6.30	7.6	9.1	18.8	22.3	21.4	14.2	6.6
119-KL	1.00–1.05	5.6	5.7	10.7	18.1	26.9	19.0	14.1
119-KL	1.55–1.60	9.9	7.6	10.6	17.3	35.0	14.8	7.4
119-KL	6.30–6.35	4.3	5.9	11.0	24.1	28.2	17.4	9.0
119-KL	9.86–9.91	10.5	11.6	20.9	27.8	18.5	6.1	4.6
120-KL	4.05–4.10	7.8	7.6	11.8	16.8	23.2	18.0	14.8

Note: size fractions (in micrometers) expressed as a percentage (weight) of the carbonate-free samples. Column 1: <0.2; 2: 0.2–0.6; 3: 0.6–2; 4: 2–6.3; 5: 6.3–20; 6: 20–63; 7: >63 μm.

Materials and methods

Samples were collected from pelagic soft sediment recovered in cores taken from various latitudes and different deep-sea environments (Table 1): (1) Deep-Sea Drilling Project (DSDP) core, south Atlantic, Angola Basin, Leg 73, (2) piston cores obtained during the FS-Sonne cruise SO-25 in the north-central Pacific, (3) piston cores obtained during the FS-Sonne cruise SO-35 in the North Fiji Basin and Lau Basin (Amarantidis, 1990). For a morphological comparison, a hydrothermal and authigenic deep-sea sediment (509B-2-1, 44–48 cm, in Barrett and Friedrichsen, 1982) from the Galapagos Spreading Center was included in our investigation.

Samples from the north-central Pacific show small variations in the proportion of their size fractions (Table 2). In addition to clay minerals, zeolite-group minerals are a major component (commonly approximately 30%). As these sediments were deposited below the carbonate compensation depth (CCD), they are virtually carbonate-free.

The composition of the samples from the Angola Basin varies from predominantly siliceous foraminiferal and nanofossil calcareous oozes to clay-rich material (Karpoff, 1984). The samples from the North Fiji and Lau Basins are carbonate-rich and composed of a mixture of volcaniclastic detritus, clay minerals, siliceous foraminiferal and nanofossil calcareous oozes. The proportion of carbonate present is given in Table 1.

Prior to size fractionation (Table 2), the samples were treated three times with a 0.1-*M* solution of the disodium salt of ethylenediamine-tetra-acetic acid (EDTA-Na_2), each time for 24 h at room temperature, to remove carbonate and to saturate the clay-mineral phases with Na. To remove the excess Na, the samples were then washed several times with deionized H_2O. The mineralogical compositions of the bulk samples and of selected coarser fractions were determined by optical microscopy, X-ray diffraction (XRD), and scanning electron microscopy (SEM) linked with an energy-dispersive spectrometer (EDX). The <0.2-μm size fraction from our 23 samples was separated with a conventional centrifuge for detailed investigations of clay-mineral phases present in these sediments, by XRD, transmission electron microscopy (TEM), and wet chemical analysis. XRD data were obtained from oriented glycerol-treated samples. The morphology and layer structure of the clay-mineral phases were studied with TEM using samples prepared by the ultramicrotome techniques of Vali and Köster (1986). The distinction between expandable and nonexpandable components was made possible with *n*-alkylammonium-treated ultrathin sections (Vali and Hesse, 1990). Chemical compositions were determined by duplicate wet-chemical analyses of the bulk <0.2-μm fraction following

the procedure described by Köster (1979). Details are provided in the footnotes to Table 3. Structural formulas (Table 4) were calculated according to the method of Köster (1977). In some cases, a semiquantitative analysis of the clay-mineral particles was performed by analytical TEM (JEOL 100 CX, equipped with an energy-dispersive X-ray detector). The iron oxides coating the surface of clay-mineral particles were removed by the dithionite-citrate method (Mehra and Jackson, 1960).

Results of XRD, TEM, and HRTEM analyses

A TEM investigation of the <0.2-μm fraction revealed the presence of abundant contaminant phases in addition to smectite-group minerals. To assess the contribution of accessory minerals (i.e., zeolites, micas, iron oxides) to the chemical composition of the <0.2-μm fraction, the mineral components in the individual size-fractions were identified by XRD and analytical SEM (Amarantidis, 1990).

XRD analyses, <0.2-μm fraction

After glycerol treatment, the XRD patterns of the <0.2-μm fraction of all 23 samples revealed basal spacings of 17–17.5 (001), 8.5–9 (002), and 3.5–3.6 Å (005), typical of smectite-group minerals. The shapes and angular positions of these peaks in samples from the Angola Basin and north-central Pacific are similar, with no significant modifications in samples taken from different depths. In contrast, patterns for the samples from the North Fiji and Lau Basins reveal the occurrence of a smectite-group phase only at a depth >3 m below the sediment surface (Fig. 1); its proportion increases from approximately 5 to 90% of the <0.2-μm fraction (TEM estimate) with increasing depth. An improvement in the quality of the above peaks with increasing depth is consistent with the formation and development of a smectite-group phase or phases in this region. Patterns for samples from shallower depths in the Lau Basin show a weak 14-Å peak, which corresponds to a chlorite-group mineral (Fig. 1a). The presence of chlorite particles was confirmed with the TEM. The pattern for the sample from 9.86–9.91 m (Table 1) shows clearly an integral series of basal (00*l*) reflections for smectite (Fig. 1c). The hump between 15 and 30° 2θ on the diffractograms (Fig. 1a–1c) probably is caused by amorphous components, whose presence is revealed by TEM (see below). The 060 reflection at approximately 1.51 Å, measured in XRD patterns for all samples, is indicative of the dioctahedral nature of the 2:1 layer silicate.

TEM images, air-dried specimens

TEM images of air-dried specimens reveal flakes with diffuse and curled edges, a feature of aggregation similar to that observed in Cheto-type montmorillonite (Güven, 1974; Vali and Köster, 1986); lath-shaped particles or filmlike aggregates similar to those observed in hectorite, nontronite, and Wyoming-type montmorillonite are not present. It is important to mention that the true morphology and size of the individual crystals of the smectite-group mineral could not be observed in the TEM with the techniques of preparation used here (see Discussion).

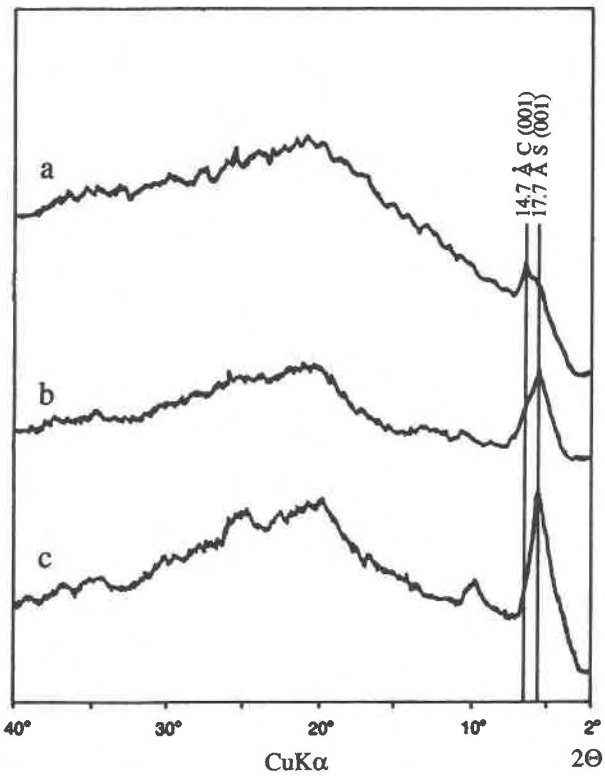

Fig. 1. XRD diagrams of the <0.2-μm fraction of sediments in the Lau Basin showing increasing development of smectite with depths. Depth of samples: (a) 100–105, (b) 630–635, (c) 986–991 cm. All three samples were treated with glycerol. Symbols: C = chlorite, S = smectite-group mineral.

In addition to the common phases illite, chlorite, kaolinite, feldspar, hematite, goethite, amorphous iron oxides, and volcanic glass, all samples of deep-sea sediment studied contain a considerable amount of biogenic magnetite (Fig. 2), which represents the fossil remains of magnetic bacteria (Blakemore, 1975; Kirschvink and Chang, 1984; Petersen et al., 1986; Vali et al., 1987). Also present in all samples are inorganic single-domain (200–1000 Å) and superparamagnetic (<200 Å) particles of titaniferous magnetite and other magnetic material (Vali et al., 1989). Furthermore, samples from the Angola Basin and north-central Pacific contain between 10 and 40% zeolites (Fig. 2). As it was not possible to separate these particles from the smectite-group components (Petersen et al., 1986; Amarantidis, 1990), it seems clear that the <0.2-μm fraction that was chemically analyzed contains a certain amount of additional Fe, Al, Si, and K, which must be considered in the calculation of the structural formula of the smectite-group mineral.

Table 3. Chemical composition of <0.2-μm fraction of deep-sea sediments*

	North-central Pacific					Angola Basin					
	1	2	3	4	5	6	7	8	9	10	11
						Weight percents					
SiO_2	46.1	46.3	46.4	47.0	47.2	48.7	48.1	48.2	48.8	49.8	48.5
Al_2O_3	15.1	14.3	14.2	13.4	13.9	16.1	15.0	12.8	14.8	12.4	11.7
Fe_2O_3	11.04	10.14	10.79	9.48	9.49	11.80	12.40	14.60	8.96	9.96	12.9
Fe_2O_3**	1.30	1.07	1.21	0.98	0.94	1.57	2.00	3.07	1.16	1.01	2.05
MgO	4.44	5.06	4.67	5.53	5.59	3.50	3.65	4.20	5.31	4.25	4.25
CaO	0.77	0.68	0.70	0.76	0.49	0.24	0.20	0.33	0.40	0.30	0.50
Na_2O	1.18	0.69	1.18	0.59	0.79	1.68	1.23	1.03	1.09	1.32	0.98
K_2O	2.08	1.60	1.69	1.42	1.42	2.89	3.01	3.43	3.25	2.77	2.71
TiO_2	0.55	0.52	0.56	0.51	0.46	0.39	0.44	0.41	0.45	0.45	0.53
						Parts per million					
Cr	68	62	64	49	47	58	42	39	40	39	38
Mn	298	331	464	296	308	260	285	482	421	346	315
Co	12	13	12	8	4	8	7	7	8	7	6
Ni	22	24	38	41	34	17	17	11	—	22	13
Cu	673	786	919	1073	944	97	134	145	87	115	105
Zn	243	305	275	305	318	248	314	314	326	291	291
Cd	<4	<4	<4	<4	<4	<3	<3	<3	<3	<3	<3
Pb	38	23	8	—	7	37	21	58	94	57	29
Li	82	99	92	126	133	69	70	58	130	72	61
Rb	149	140	148	131	131	144	140	140	117	117	112
Sr	<40	<40	<40	<40	<40	49	81	68	139	63	94
Ba	—	—	—	—	—	118	134	—	—	—	—
P	68	35	43	32	31	21	288	245	94	20	68

	North Fiji Basin				Lau Basin				
	12	13	14	15	16	17	18	19	20
					Weight percents				
SiO_2	41.3	42.5	47.4	39.9	36.9	45.7	45.4	34.3	34.8
Al_2O_3	14.8	15.9	11.0	15.5	10.0	8.7	10.3	8.5	10.1
Fe_2O_3	14.70	14.60	13.30	14.00	24.80	10.40	10.80	25.40	25.70
Fe_2O_3**	4.70	4.68	4.70	5.79	14.98	2.67	1.68	15.6	15.1
MgO	2.97	3.24	3.92	3.05	1.68	0.25	0.32	1.68	2.12
CaO	1.03	0.62	0.50	0.92	1.10	0.19	0.20	1.43	1.45
Na_2O	0.56	0.85	1.69	0.66	1.17	0.24	0.22	1.01	0.97
K_2O	0.75	0.46	0.48	0.37	0.42	1.08	0.48	0.46	0.44
TiO_2	0.79	0.70	0.39	0.70	0.82	0.54	0.62	0.85	0.84
					Parts per million				
Cr	—	—	60	77	80	—	—	79	63
Mn	526	1099	4564	1905	3721	—	—	14722	2358
Co	<10	<10	7	25	14	—	—	48	8
Ni	<40	<40	39	45	40	—	—	29	40
Cu	257	452	526	332	384	1357	2488	290	252
Zn	184	237	279	246	296	540	436	483	531
Cd	<10	<10	3	1	<3	—	—	6	<3
Pb	25	43	57	74	126	—	—	765	104
Li	82	88	99	94	23	3	5	24	22
Rb	51	51	33	37	31	9	9	33	31
Sr	181	194	109	352	482	42	10	655	542
Ba	<400	<400	—	—	—	—	—	—	—
P	660	539	275	546	3380	1138	240	3097	8787

* The <0.2-μm fraction subjected to chemical analysis is Na-saturated and carbonate-free. In the above, — means "not determined." Samples from the north-central Pacific (drill core, depth): (1) 133-KL, 4.60–4.65 m; (2) 177-KL, 3.10–3.15 m; (3) 184-KL, 8.00–8.05 m; (4) 314-KL, 5.20–5.25 m; (5) 383-KL, 2.40–2.45 m. Samples from the Angola Basin: (6) 522, 37–41 m; (7) 522, 51–55 m; (8) 522, 140–148 m; (9) 523, 93–99 m; (10) 523, 131–135 m; (11) 523, 160–167 m. Samples from the North Fiji Basin: (12) 182-KL, 2.75–2.80 m; (13) 182-KL, 5.10–5.14 m; (14) 182-KL, 12.45–12.5 m; (15) 184-KL, 6.02–6.07 m. Samples from the Lau Basin: (16) 119-KL, 1.00–1.05 m; (17) 119-KL, 6.30–6.35 m; (18) 119-KL, 9.86–9.91 m; (19) 110-KL, 6.25–6.30 m; (20) 120-KL, 4.05–4.10 m.

** Dithionite-extractable iron oxide (the amorphous fraction). The concentrations of major and minor elements were determined as follows: Si, Al, Fe, Ti, Mn, P, Pb, Ni, and Cr by spectrophotometry, Na, K, Li, Rb, Sr, Co, and Cd by flame emission spectroscopy, and Mg, Ca, Ba, Cu, and Zn by atomic absorption spectroscopy (methods of Köster, 1979).

HRTEM imaging, *n*-alkylammonium-treated ultrathin sections

In ultrathin sections, the smectite-group mineral displays random stacks of 2:1 layer silicate with a spacing of 12–13 Å. The degree of stacking order in the layer structure in the sediments from the north-central Pacific and the Angola Basin was found to be very constant as a function of depth. In contrast, samples from shallower depths in the North Fiji and Lau Basins do not show a coherent stacking order in the layer structure. Single lay-

Table 4. Calculated structural formulas of dominant smectite-group mineral

	Tetrahedral sites			Octahedral sites				Interlayer				
	Si	$^{[4]}$Al	Charge	$^{[6]}$Al	Fe^{3+}	Mg	Charge	Ca	Na	K	CEC	Charge
North-central Pacific 1												
383-KL	4.04	—	16.16	1.35	0.00	0.77	5.61	0.05	0.14	0.00	—	0.23
177-KL	3.99	0.01	15.99	1.43	0.00	0.73	5.74	0.07	0.13	0.00	—	0.27
133-KL	3.94	0.06	15.94	1.45	0.00	0.66	5.67	0.08	0.23	0.00	—	0.39
315-KL	4.04	—	16.16	1.34	0.00	0.79	5.58	0.08	0.11	0.00	—	0.26
184-KL	4.00	0.00	16.00	1.42	0.00	0.68	5.63	0.07	0.23	0.00	—	0.37
North-central Pacific 2												
383-KL	4.03	0.00	16.13	1.35	0.00	0.77	5.60	—	—	—	0.27	0.27
177-KL	3.96	0.04	15.96	1.40	0.00	0.73	5.65	—	—	—	0.39	0.39
133-KL	3.94	0.06	15.94	1.45	0.00	0.66	5.69	—	—	—	0.37	0.37
315-KL	4.05	—	16.20	1.34	0.00	0.79	5.60	—	—	—	0.20	0.20
184-KL	3.99	0.01	15.99	1.41	0.00	0.68	5.59	—	—	—	0.43	0.43
North-central Pacific 3												
177-KL	3.89	0.11	15.89	1.29	0.14	0.71	5.73	—	—	—	0.38	0.38
133-KL	3.86	0.14	15.86	1.34	0.15	0.65	5.78	—	—	—	0.36	0.36
Angola Basin												
522 c10	3.91	0.09	15.91	0.74	0.80	0.54	5.69	0.03	0.34	0.00	—	0.40
522 c14	3.99	0.01	15.99	0.65	0.85	0.59	5.71	0.02	0.26	0.00	—	0.30
523 c37	4.00	0.00	16.00	0.77	0.69	0.65	5.67	0.03	0.26	0.00	—	0.33
North Fiji Basin												
182-KL	4.00	0.00	16.00	0.97	0.57	0.51	5.62	0.05	0.29	0.00	—	0.38

Note: for samples from the north-central Pacific, structural formulas were calculated in three ways: (1) K and Fe were not considered to be structurally bound in the clay, but rather present as impurity phases; (2) the measured value of cation-exchange capacity (CEC) was used in the calculation of the structural formula, and (3) 2–3% of the Fe_{tot} was considered to be octahedrally coordinated in the layer silicate. For three samples from the Angola Basin and one from the North Fiji Basin, all the K and that part of the Fe present in the form of amorphous iron oxide were not considered in the calculation of the structural formula. In the case of three samples from the Angola Basin, the remaining samples from the North Fiji Basin, and all samples from the Lau Basin, it has not been possible to calculate a reliable structural formula.

ers or thin, disrupted stacks of a few smectitic layers were observed in association with clusters of particles 50–100 Å across (Fig. 3a). This material does not show any pattern in selected-area electron diffraction. Samples from deeper sediments have a more perfect degree of stacking order and seem to have a coarser grain size (Fig. 3b). With the exception of samples from the Angola Basin, most of the samples studied do not contain illite-smectite or chlorite-smectite mixed layers. In addition to the smectite-group phases, samples from the Angola Basin examined by TEM after alkylammonium treatment show random mixed-layer arrays of expandable and nonexpandable interlayers (Fig. 4a, 4b). Small domains (units?) of layers with nonexpanded interlayers occur within smectitic layers. There also is a considerable proportion of two-layer units with a single nonexpanded interlayer (see caption to Fig. 4). In contrast to the smectitic interlayers, the interlayer charge density of these domains is sufficiently high to fix K^+ so that it cannot even be depleted by octadecylammonium ion treatment ($C_{n=18}$). The proportion of K^+ associated with these domains cannot be determined directly because of the limitation of the analytical TEM. However, it is most likely that all of the K^+ present in the sample is associated with interlayers of the nonexpandable (illitic?) components, since the amount of K^+ does not change significantly after *n*-alkylammonium treatment. Individual packets of illite layers also were observed as discrete phases (Vali et al., 1991). A similar structure also was observed in the authigenic deep-sea sediment (509B-2-1, 44–48 cm) from the Galapagos Spreading Center. Clay minerals associated with the hydrothermal mounds were described as glauconite, celadonite, nontronite, "Fe-smectite," and "Fe-montmorillonite," present as discrete phases (McMurtry et al., 1983; Honnorez et al., 1983; Buatier et al., 1989). Our TEM results on ultrathin sections from untreated granules reveal three types of layer structures: (1) discrete smectitic layers, (2) discrete packets of nonexpandable 10-Å layers, and (3) mixed-layer structures formed of 1 and 2 (Fig. 5a–5c).

The chemical composition and structural formula of the dominant smectite-group mineral

North-central Pacific

The chemical composition of the <0.2-μm fractions of Na-saturated and carbonate-free samples is given in Table 3. Samples from the north-central Pacific, collected from different cores and at various depths, revealed no significant variations in the concentration of both major and minor elements (Table 3). On the basis of results of our TEM investigation, these samples contain abundant biogenic magnetite (see above) and phillipsite (the absence of Ba indicates that harmotome, present in coarser fractions, does not occur in the <0.2-μm fraction).

Since the results of a bulk analysis cannot be used directly to calculate the structural formula of the smectite-

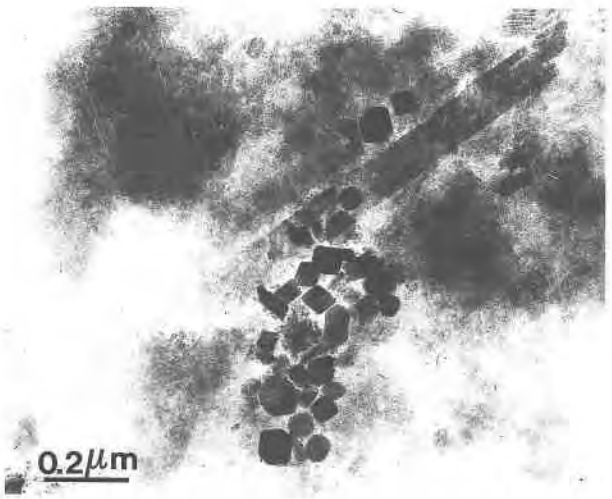

Fig. 2. TEM images of an air-dried specimen of the <0.2-μm fraction from the north-central Pacific showing aggregates of montmorillonite, together with crystals of phillipsite (laths) and magnetite (small particles in the center).

group phase, we attempted to correct the chemical data by removing the contribution from the obvious contaminating phases. As a first approach, the entire proportion of Fe determined was considered to be derived from magnetite; the entire amount of K and an equivalent amount of Si and Al were removed as phillipsite, in agreement with the empirically derived average composition $[K_{4.5}Al_{4.5}Si_{23}O_{46} \cdot 20H_2O]$. The composition of the phillipsite in our samples thus is found to be very similar to that from various deep-sea regions investigated by Sheppard et al. (1970) and Stonecipher (1978). After these corrections, the calculated structural formulas for five samples from the north-central Pacific are found to match closely the ideal composition for montmorillonite (Table 4, North-central Pacific 1). In these calculations, the Na and Ca determined by analysis are considered to be present as exchangeable cations in the interlayer position. However, when the samples are treated with 0.1-*M* EDTA-Na_2, the exchangeable Ca is expected to be replaced by Na. Therefore, an attempt was made to calculate the structural formulas of the same five samples based on the cation-exchange capacity (CEC) data (Table 4, North-central Pacific 2). Although the measured CEC data were corrected for the phillipsite contaminant, the layer charges seem to be larger than those calculated from the amount of Ca and Na determined by chemical analysis in the first calculation (except for sample 315-KL). One reason for this discrepancy could be the broad variation in the cation-exchange capacity of the zeolite impurity (200–400 meq per 100 g: Flanigen and Mumpton, 1977) and the presence of some illitic material in these samples. In two samples, a charge balance also was achieved by considering 2–3% of the amount of Fe as an octahedrally coordinated cation (Table 4, North-central Pacific 3). The addition of Fe to the smectite structure resulted in a greater proportion of Al substituting for Si in the tetrahedral position.

Angola Basin

The chemical composition of samples from the Angola Basin (Table 3) shows no significant variation in Si con-

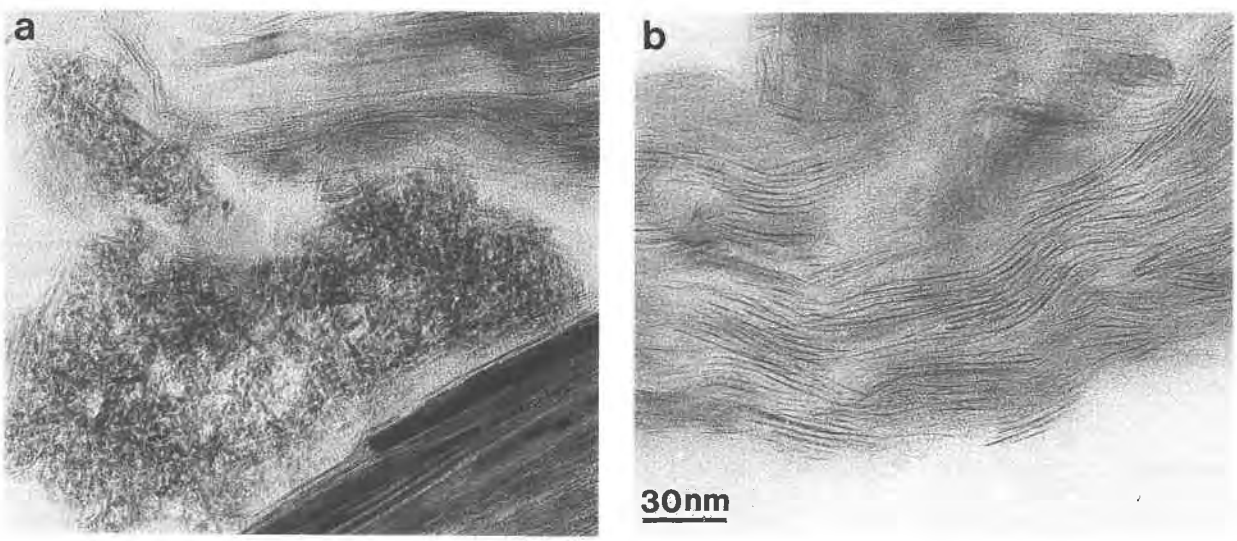

Fig. 3. TEM images of ultrathin sections of the <0.2-μm fraction of sediments in the Lau Basin: (**a**) amorphous material, together with some smectite layers and possibly chlorite, (black lath at the lower right corner) representing the features of the samples from the shallowest depth (119-KL 1.00–1.05 m). (**b**) Layer structure of sample 119-KL (9.86–9.91 m) representing the morphology of a well-crystallized smectite-group mineral in this region and typical of the north-central Pacific and the North Fiji Basin. Sample shown in **b** was treated with octadecylammonium ions. The spacing of the lattice fringes of the smectite-group mineral varies between 20 and 30 Å. Scale bar is the same in both photos.

tent; on the other hand, some variation does occur in the concentration of the other major elements. Samples from core 522 contain less Al, with concomitantly higher Fe, Mg, and K the deeper the sample. Samples from core 523 show a decrease in amount of Al, Mg, and K with depth, whereas the Fe content increases. The K belongs to an illitic component present in these samples. Nonexpandable 10-Å layers containing K were evident in the TEM after *n*-alkylammonium treatment (Fig. 4a–4c). Therefore, in calculating the structural formula of the smectite-group phase, the entire amount of K and an equivalent amount of Si and Al were removed according to the ratio in ideal muscovite. We used ideal muscovite because the exact composition of the nonexpandable, probably illitic, component is not known. In contrast to the samples from the north-central Pacific, the <0.2-μm fraction contains a much lower amount of phillipsite than of illite. Thus zeolite-group minerals here may not be a significant contaminant. Since the concentration of biogenic magnetite in these samples is much lower than that observed in the samples from the north-central Pacific (Fig. 2), only the amount of Fe considered present as amorphous iron oxides (i.e., dithionite-extractable) was subtracted. These corrections led to a reliable structural formula for three

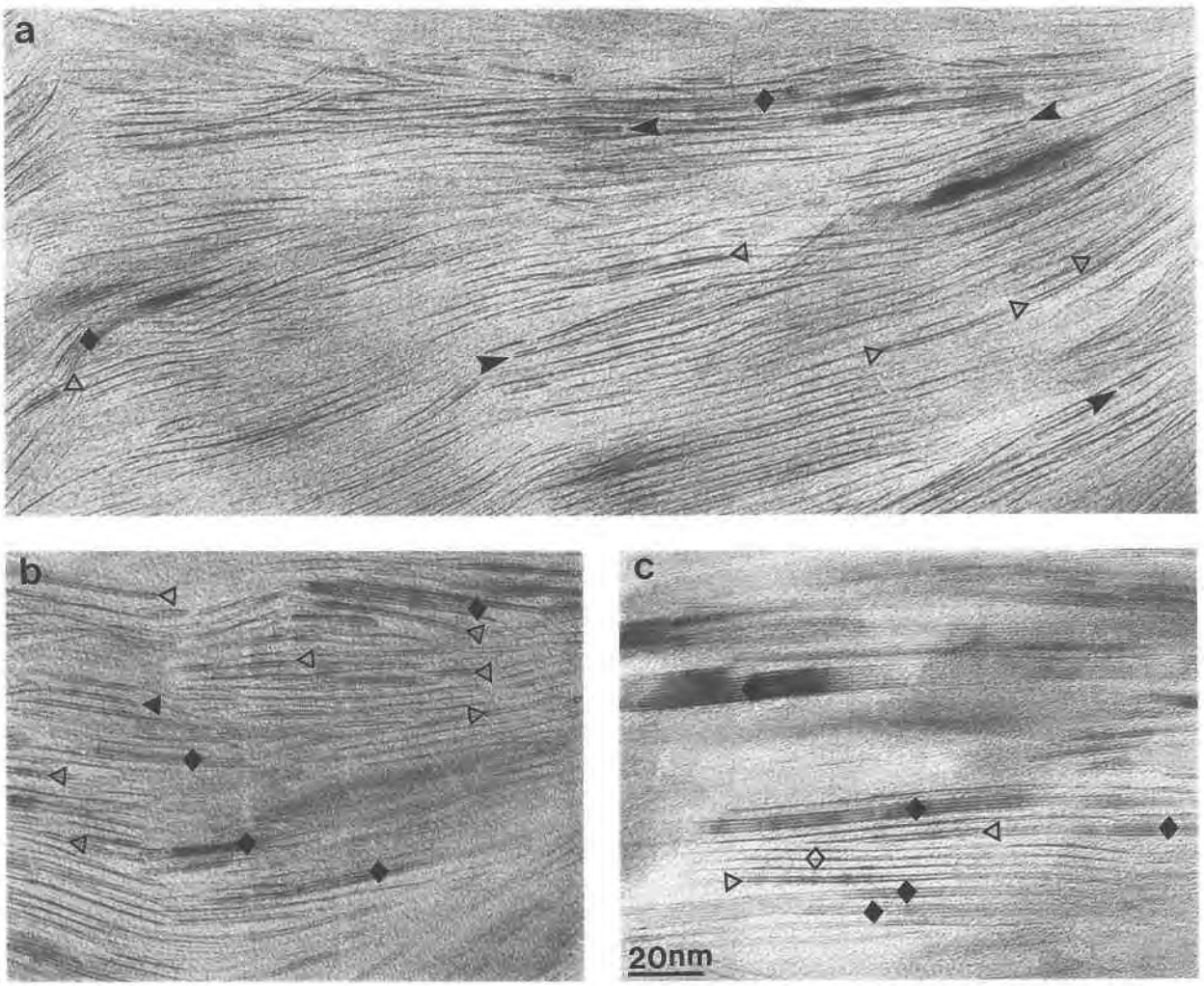

Fig. 4. TEM images of aggregates in one octadecylammonium-treated ultrathin section of the <0.2-μm fraction of the sample 522 (51–55 m) from Angola Basin showing the different types of layer structures occurring in this sample that are typical of this region: (**a**) single layer and stacks of smectite layers (spacing of 20–30 Å) containing some nonexpandable layers of illite (10 Å). Black arrows show an early stage in the development of double layers (open triangles), which eventually form an $R = 1$ ordered structure (black triangles in **b**). The image is representative of 85% of the sample. (**b**) In these aggregates, the proportion of double-layer (open triangles) and illite units (black diamonds) is greater. (**c**) Packets of discrete nonexpandable (10 Å, black diamonds) and expandable (~24 Å, open diamond) illites (see Vali et al., 1991). From the evidence presented here, the smallest unit of illite involves three layers. The double layer (open triangles in **a** and **b**) described by Nadeau et al. (1984) as the fundamental particle for illite is in fact the smallest unit for the $R = 1$ ordered structure. Scale bar is the same in all three photos.

Fig. 5. (**a–c**) TEM images of aggregates in one octadecylammonium-treated ultrathin section of the original (i.e., without pretreatment) sample (509B-2-1, 44–48 cm) from the Galapagos Spreading Center, showing different types of layer structures. In general, the morphological features are similar to those illustrated in Fig. 4, except that the open diamonds refer to layers of nontronite in nonparallel stacking and random spacing (13–30 Å). The nonexpandable component consists of celadonite or glauconite (Buatier et al., 1989). Symbols in **b** and **c** have the same significance as in Fig. 4. Scale bar is the same in all three photos.

of the samples from this region (Table 4, Angola Basin). Although the charge distribution indicates an ideal montmorillonite bulk composition for these samples, it is likely that some of the $^{[6]}$Fe reflects the presence of an iron oxide impurity (biogenic magnetite).

North Fiji Basin and Lau Basin

As for samples from the North Fiji Basin and Lau Basin (Table 3), calculation of the structural formula was possible only for sample 182-KL (12.45–12.50 m) after removing (1) all of the K and an equivalent amount of Si and Al as muscovite, and (2) the dithionite-extractable Fe from the bulk chemical compositions (Table 4, North Fiji Basin). Note that the Fe_{tot} content of the samples in these two regions is apparently higher than in samples from the north-central Pacific and Angola Basin. However, this difference is the result of greater amounts of amorphous, dithionite-extractable Fe present in these samples (Table 3). Surprisingly, all 23 samples are very similar in Fe content after dithionite treatment. The low Fe content of samples 17 and 18 is due to the dithionite treatment prior to size fractionation. These two samples were not dispersed by treatment with EDTA-Na_2. The

chemical composition of these two samples, compared with the other sample from the same core (Table 3), shows that the dithionite treatment removes not only the amorphous iron oxide, but also other major and minor elements, such as Ca, Mg, Na, Li, Sr, Rb, and Mn.

The samples of core 182-KL from the North Fiji Basin (Table 3) reflect a depth-dependent correlation among elements, such that Al and Fe decrease and Si and Mg increase with increasing depth. The atomic proportions in the deeper samples are close to those of end-member montmorillonite (Table 4, North Fiji Basin). This is also supported by TEM observations, which reveal the formation and development of a smectite-group mineral in the deeper samples along core 182-KL.

Trace-element concentrations

The trace elements in the individual samples from different regions do not vary much in relative concentration, except for a relatively high concentration of Cu and Zn in the samples from the Lau Basin (Table 3). Also, there are no significant correlations between the trace and major elements. However, it is obvious that most of the alkali, alkaline earth, and trace elements, except for K, Cu, and Zn, are removed by the dithionite treatment (Table 3, samples 17, 18). These elements thus are either present as exchangeable cations associated with the smectite-group mineral or associated with the accessory minerals present. It is also evident that K^+ occurs as a fixed cation rather than as an exchangeable cation.

Discussion

A mineralogical and geochemical investigation of 23 deep-sea samples from four regions has revealed the significance of accessory minerals and other contaminants in the characterization of the smectite-group mineral present. Based on XRD results, only a smectite-group mineral is expected to be dominant in the <0.2-μm fraction. However, other mineral phases such as iron oxides, illite, chlorite, and phillipsite are observed in the TEM. The proportion of these accessory minerals increases considerably with increasing size fraction (Amarantidis, 1990). Thus it seems evident that data on bulk samples of the >0.2-μm fractions, as reported in the literature, are likely to be of little use in the determination of the structural formulas of smectite-group minerals, as they are likely to pertain to a mixture of clay minerals and various contaminants. Unfortunately, in most cases the contribution of contaminants has been ignored in the characterization of clay minerals occurring in deep-sea sediments.

In any chemical characterization of clay-mineral phases, contributions of the contaminants and analytical error must be considered. Size fractionation and chemical pretreatment are useful procedures to facilitate the separation of phases and the removal of accessory minerals in the clay fractions (McMurtry et al., 1983; Ohr et al., 1990). However, great care is required during centrifugation and sample preparation. In most cases, the use of a conventional centrifuge or the Sharples continuous-flux ultracentrifuge results in contamination of the desired size fractions with larger particles. Usually, the concentration of these contaminants is below the detection limit of XRD. Therefore, the purity of the individual fractions must be assessed by TEM. AEM techniques may be applied to identify the contaminants and to estimate their concentration. Chemical pretreatment (e.g., dithionite, HCl, H_2O_2) for the removal of organic and amorphous components clearly alters the chemical composition of the samples, as seen by the dithionite-citrate treatment of the samples from the Lau Basin (Table 3, samples 17, 18). Furthermore, contaminants such as quartz, feldspars, and magnetite cannot be removed by such treatment.

The clay fractions of deep-sea sediments generally contain significant Fe and K. Since the XRD patterns indicate the presence of a smectite-group mineral only, all the Fe and K recorded in the analysis typically are included in the structural formula of a monomineralic species, considered a smectite (e.g., Hein et al., 1979; Hoffer et al., 1980; Honnorez et al., 1983; Karpoff, 1984; Singer et al., 1984; Buatier et al., 1989). Using data derived from bulk chemistry, Hein et al. (1979) described samples from the north-central Pacific as being Fe-rich smectite, and Karpoff (1984) identified samples from the Angola Basin as containing beidellite and nontronite. However, a TEM investigation provides clear evidence that the K determined in all our samples is mostly associated with the contaminants. The amount of K in the <0.2-μm fraction correlates with the amount of K estimated from the proportion of phillipsite and illite present in the samples. Therefore, bulk analytical data obtained on the <0.2-μm fraction of sediments from both regions (Table 3), corrected for the presence of accessory minerals and other contaminants (Table 4), reveal a structural formula very close to that of ideal montmorillonite.

If K is considered as an interlayer cation, the reported layer charge of smectite-group minerals from recent deep-sea sediments, including hydrothermal nontronite (Hoffer et al., 1980; McMurtry et al., 1983; Buatier et al., 1989), is systematically too high. Buatier et al. (1989) reported the authigenic formation of glauconite and smectite-group phases in deep-sea sediments from the Galapagos Spreading Center. On the basis of analytical data on individual particles from a deep-sea sediment obtained with the analytical TEM, they described their smectite-group minerals as Fe-rich smectite (nontronite and "Fe-montmorillonite") and assigned the entire amount of K as an interlayer cation. TEM images of *n*-alkylammonium-treated ultrathin sections of samples from the same sediments (509B-2-1, 44–48 cm) reveal that the K present in these samples is mostly derived from the nonexpandable component (celadonite or glauconite?), made visible by the treatment (Fig. 5a–5c). The dimension of expandable and nonexpandable domains is much smaller than that of the smectite-like particles of Buatier et al. (1989). Thus their particles may not represent sin-

gle-phase clay minerals, but rather aggregates consisting of more than one clay-mineral phase, as well as a coating and amorphous material. The variability in chemical composition of individual particles among the same type of samples (Table 2 in Buatier et al., 1989) provides clear evidence for such heterogeneity.

The dimension of units composed of distinct layers within the clay-mineral mixtures is smaller than the diameter of the electron beam used in analytical electron microscopy (AEM). The chemical composition of discrete phases can only be studied in a dispersion. The true dimension of individual particles of the smectite-group phases in dispersion can be studied with TEM using freeze-etch techniques (Vali and Bachmann, 1988; Vali and Hesse, 1992a). From TEM observation of the ultrathin sections of samples from Angola Basin and the Galapagos mounds, the dimensions of individual domains seem about the same as those of smectite-group minerals illustrated in these two articles. Thus the true layer-structure and chemistry of mixed-layer clay minerals can only be studied in dispersion using cryo-ultramicrotomy and cryomicroscopy techniques (Zierold, 1987). Although application of the AEM is the best approach in analyzing individual mineral phases, including clay minerals (Buatier et al., 1992), the resolution of the electron beam and the analytical precision in AEM are inadequate for the reliable analysis of the smallest particles (Warren and Ransom, 1992; Banfield et al., 1991; Peacor, 1992a).

Although the calculated structural formulas (Table 4) are close to the formula of ideal montmorillonite, the reliability of a classification scheme of clay minerals based solely on chemical composition remains to be established. Small variations in the chemical data result in drastic changes in the inferred stoichiometry of the smectite-group mineral (Köster, 1977; Warren and Ransom, 1992). For example, addition of 2% Fe_2O_3 to the structure (Table 4, North-central Pacific 3) results in significant changes in the occupancies of tetrahedrally and octahedrally coordinates sites. The presence of amorphous Si and Al may explain the excess positive charge associated with the sheet of tetrahedra.

The layer charge derived from the concentration of Na and Ca or from CEC values is a measure of the mean negative charge on the whole sample but does not necessarily reflect the actual layer charge of the smectite-group mineral. A more reliable assessment of interlayer charge can be achieved by the *n*-alkylammonium method (Lagaly and Weiss, 1969), which measures the true charge density associated with the interlayers in individual smectite-group minerals. Unfortunately, the amount of sample required for this technique (approximately 500 mg) is not always available, especially in samples of deep-sea sediments. In addition, possible errors associated with the chemical analysis and with the data-reduction procedure also must be considered. Thus, the suggested formula can be seen as an approach but may not correspond to the actual structural composition of an individual smectite-group mineral occurring in deep-sea sediments.

The extensive chemical variability in minerals of the smectite group usually is attributed to solid solution in these minerals (Velde, 1985; Velde and Brusewitz, 1986; Velde and Meunier, 1987; Newman and Brown, 1987); if so, all three calculated formulas of the smectite-group phase in samples from the north-central Pacific (Table 4) thus could be valid. It is obvious that the end-member smectite-group minerals nontronite and montmorillonite indeed are found in cases where the precursor material was homogeneous and where authigenic formation is evident, as in sediments from the north-central Pacific (Hein et al., 1979) and the Galapagos hydrothermal mounds (McMurtry et al., 1983; Buatier et al., 1989). Samples having both Al and Fe in the structure, as seen in Fe-rich montmorillonite from the Angola and North Fiji Basins (Table 4) or Fe-rich montmorillonite reported from pelagic ooze in Galapagos mounds (McMurtry et al., 1983) and other so-called Fe-smectites, also could be described as single phases.

The phase definition and thermodynamic status of 2:1 phyllosilicates remains an unsettled issue in the literature. The solubility studies of May et al. (1986) confirm the model of Lippmann (1982), that smectite-group minerals do not form in stable equilibrium; they form by precipitation from supersaturated solutions. On the other hand, on the basis of findings in other studies of solubility, smectite-group minerals have been interpreted as products of an equilibrium process whose chemical composition reflects the environment of formation (Kittrick and Peryea, 1988, 1989; Aja and Rosenberg, 1992). Clearly, resolution of this dilemma is beyond the scope of this paper. The variation in chemical composition, which is the basis of the above discussion, may also reflect (1) the occurrence of mixed-layer structures, (2) the presence of compositionally distinct domains in the structure, and (3) a mixture of two or more distinct phases.

A clear distinction between the monomineralic solid-solution phase and the mixtures of the end-members based on chemical composition or even conventional XRD and HRTEM techniques is of crucial importance. For example, samples having both Al and Fe in the structural formula could also be interpreted as a mixture of two or more phases instead of as a single solid phase. The formation of a mixture can be explained simply by the simultaneous occurrence of authigenic and detrital smectite-group phases in a sediment, or by the presence of different precursor minerals. Karpoff (1984) suggested that smectite-group minerals of detrital and authigenic origins are present in the sediments of the Angola Basin. McMurtry et al. (1983) also described Fe-rich montmorillonite from Galapagos Spreading Center as a mixture of authigenic "Fe-montmorillonite" and detrital "Al-montmorillonite." Formation of two or more smectite-group phases under conditions of local equilibrium in a microenvironment (or microsystem: Velde and Meunier, 1987) within individual precursor grains such as plagioclase and volcanic glass also is possible. Banfield et al. (1991) demonstrated the extensive compositional variations in

smectite-group minerals as a function of composition of the minerals replaced within the same sediments. Since the sediments from the Lau and North Fiji Basins contain a considerable amount of volcanic and pyroclastic detritus, it is possible that the structural formula of montmorillonite in sample 182-KL from North Fiji (Table 4) represents a mixture of two end-member smectite-group minerals (Fe-rich and Al-rich montmorillonite), which each formed under conditions of local equilibrium within different precursor minerals. Although there are no data available concerning the origin of smectite-group minerals in the North Fiji and Lau Basins, our XRD and TEM investigation of the <0.2 μm-fraction suggests that smectite-group minerals developed in situ. Slight decreases in the amounts of Al and K with a concomitant increase in the amount of Mg with depth seem to favor the authigenic model of formation of montmorillonite.

A test of the solid-solution model proposed by some could come from the study of suitably contaminant-free material by extended X-ray absorption fine structure (EXAFS). The technique has been applied successfully to trioctahedral phyllosilicates, the study of which is more straightforward than that of dioctahedral analogues because of the lack of vacant sites. Manceau (1990) has found clear evidence of the clustering of octahedrally coordinated cations in Ni-Mg and Fe-Mg trioctahedral 2:1 layer silicates earlier considered to be true solid solutions. Further departures from random occupancy are expected in F-bearing Fe-Mg layer silicates, owing to the Fe-F avoidance rule (Manceau et al., 1990; Mason, 1992). The inferred clustering of like octahedrally coordinated cations led Manceau (1990) to a reassessment of some purported examples of a monocrystalline solid-solution phase as a fine intergrowth of two end-member phases. The different response of domains in phlogopite and biotite to the *n*-alkylammonium expansion (Vali and Hesse, 1992b; Vali et al., 1992) also may be a result of the clustering of octahedrally coordinated cations. An added reason to question the presence of complex solid-solution phases in such a low-temperature environment as the sea floor is the principle of minimization of internal free energy, to be achieved by the clustering of like octahedrally coordinated atoms into relatively simple end-member structures, thus ensuring reduction in the contribution of entropy of mixing terms to the formulation of free energy.

An additional problem arises with the compositional changes attributable to weathering or diagenetic alteration. For instance, in contrast to the examples of recent and authigenic marine nontronite and glauconite, which are poor in Al (McMurtry et al., 1983; Buatier et al., 1989), terrestrial and diagenetic glauconite and nontronite contain a considerable amount of Al (Eggleton, 1977; Odin and Matter, 1981; Köster, 1982; Ireland et al., 1983). Ireland et al. (1983) suggested that the substitution of Al for Fe in these minerals is a result of progressive burial-induced diagenesis. Velde (1985) suggested the existence of two evolutionary groups of nontronite and described the Al-poor nontronite as potassic and the Al-rich one as calcic. Nontronite is considered to be the Fe-bearing analogue of beidellite, with the same structure and degree of substitution of Al for Si in the tetrahedral site (Brindley, 1980; Güven, 1988; Chamley, 1989). However, submarine authigenic samples of nontronite (McMurtry et al., 1983; Buatier et al., 1989) reveal a more montmorillonite-like formula, i.e., one that shows no significant substitution of Al for Si. A montmorillonite-like formula also has been reported for some examples of terrestrial nontronite (Hundsangen nontronite: Vali and Köster, 1986). In terms of the charge distribution and the extent of isomorphous substitutions, Al-poor nontronite, montmorillonite, and Fe-rich montmorillonite plot in the montmorillonite field on the muscovite-celadonite-pyrophyllite diagram (Köster, 1982). Consequently, a mixture of these distinct phases would mimic a smectite-group solid phase with the substitution of Al for Fe, which also would plot in the same field as smectite-group end-members. The same hypothesis is valid for the case of Al-rich nontronite vs. beidellite.

An accurate identification of clay minerals is absolutely essential to the understanding of the mechanisms of formation and development of the layer silicates in diagenetic, metamorphic, and weathering environments. In agreement with Ransom and Helgeson (1989), our study shows that the data presented in the literature concerning the classification of minerals of the smectite group and related I/S mixed layers do not necessarily reflect the true nature of the individual clay-mineral phases. A combination of thermodynamic and solubility studies (May et al., 1986; Rosenberg et al., 1990; Aja et al. 1991a, 1991b; Aja and Rosenberg, 1992; Tardy and Duplay, 1992) and detailed mineralogical investigations (e.g., Vali et al., 1991; Peacor, 1992b; Vali et al., unpublished manuscript) will be required to clarify the status of 2:1 phyllosilicates. So far in the literature, "illite-smectite" has been assigned a defined structure such as ISIS (R1 ordered), ISIIISII (R3 ordered), and end-member illite. However, use of a group name such as "smectite" or "illite" to describe a single phase obviously is misleading. The individual components in a mixed-layer structure must be determined, and the material classified by a mineral name such as rectorite and corrensite.

Acknowledgments

Helpful discussions with L. Bachmann, H.M. Köster, and R. Hesse are gratefully acknowledged. This research was supported by grants from the Deutsche Forschungsgemeinschaft (DFG), Germany, the Natural Sciences and Engineering Research Council (NSERC) of Canada, and the Petroleum Research Fund, administered by the American Chemical Society (ACS) awarded to R. Hesse. We are grateful to Tim Barrett for the samples from the Galapagos Spreading Center. We greatly appreciate the reviews of R.L. Freed and an anonymous reviewer. Samples from the north-central Pacific, North Fiji Basin, and Lau Basin were provided by the Bundesanstalt für Geowissenschaften und Rohstoffe, Hannover, Germany.

References cited

Aja, S.U., and Rosenberg, P.E. (1992) The thermodynamic status of compositionally-variable clay minerals: A discussion. Clays and Clay Minerals, 40, 292–299.

Aja, S.U., Rosenberg, P.E., and Kittrick, J.A. (1991a) Illite equilibria in solutions. I. Phase relationships in the system K_2O-Al_2O_3-SiO_2-H_2O between 25° and 250°C. Geochimica et Cosmochimica Acta, 55, 1353–1364.

——— (1991b) Illite equilibria in solutions. II. Phase relationships in the system K_2O-MgO-Al_2O_3-SiO_2-H_2O. Geochimica et Cosmochimica Acta, 55, 1365–1374.

Amarantidis, G. (1990) Sedimentpetrographische und magnetomineralogische Untersuchungen an Tiefsee-Sedimenten aus dem Pazifik und Süd-Atlantik. Ph.D. dissertation, Fakultät für Chemie, Biologie und Geowissenschaften, Technische Universität München, Germany.

Banfield, J.F., Jones, B.F., and Veblen, D.R. (1991) An AEM-TEM study of weathering and diagenesis, Albert Lake, Oregon. I. Weathering reactions in the volcanics. Geochimica et Cosmochimica Acta, 55, 2781–2793.

Barrett, T.J., and Friedrichsen, H. (1982) Elemental and isotopic composition of some metalliferous and pelagic sediments from the Galapagos mounds area, DSDP Leg 70. Chemical Geology, 36, 275–298.

Blakemore, R.P. (1975) Magnetotactic bacteria. Science, 190, 217–238.

Brindley, G.W. (1980) Order-disorder in clay mineral structures. In Mineralogical Society Monograph, 5, 125–195.

Buatier, M., Honnorez, J., and Ehret, G. (1989) Fe-smectite–glauconite transition in hydrothermal green clays from the Galapagos Spreading Center. Clays and Clay Minerals, 37, 532–541.

Buatier, M.D., Peacor, D.R., and O'Neil, J.R. (1992) Smectite-illite transition in Barbados accretionary wedge sediments: TEM and AEM evidence for dissolution/crystallization at low temperature. Clays and Clay Minerals, 40, 65–80.

Chamley, H. (1989) Clay sedimentology, 623 p. Springer-Verlag, Berlin.

Eggleton, R.A. (1977) Nontronite: Chemistry and X-ray diffraction. Clay Minerals, 12, 181–194.

Flanigen, E.M., and Mumpton, F.A. (1977) Commercial properties of natural zeolites. In Mineralogical Society of America Reviews in Mineralogy, 4, 165–175.

Güven, N. (1974) Electron-optical investigations on montmorillonites. I. Cheto, Campberteaux and Wyoming montmorillonites. Clays and Clay Minerals, 22, 155–165.

——— (1988) Smectite. In Mineralogical Society of America Reviews in Mineralogy, 19, 497–559.

Hein, J.R., Yeh, H.W., and Alexander, E. (1979) Origin of iron-rich montmorillonite from the manganese nodule belt of the North Equatorial Pacific. Clays and Clay Minerals, 27, 185–194.

Hoffer, M., Person, A., Courtois, C., Karpoff, A.M., and Trauth, D. (1980) Sedimentology, mineralogy and geochemistry of hydrothermal deposits from holes 424, 424A, 424B and 424C (Galapagos Spreading Center). In Initial Reports Deep Sea Drilling Project, 54, 339–376.

Honnorez, J., Karpoff, A.M., and Trauth-Badaut, D. (1983) Sedimentology, mineralogy and geochemistry of green clay samples from the Galapagos hydrothermal mounds, holes 506, 506C, and 507D Deep Sea Drilling Project Leg 70. In Initial Reports Deep Sea Drilling Project, 70, 221–224.

Ireland, B.J., Curtis, C.D., and Whiteman, J.A. (1983) Compositional variation within some glauconite and illites and implication for their stability and origins. Sedimentology, 30, 769–786.

Karpoff, A.M. (1984) Miocene red clays of the South Atlantic: Dissolution facies of calcareous oozes at Deep Sea Drilling Project sites 516 to 523, Leg 73. In Initial Reports Deep Sea Drilling Project, 73, 515–535.

Kirschvink, J.L., and Chang, S.R. (1984) Ultrafine-grained magnetite in deep-sea sediments: Possible magnetofossils. Geology, 12, 559–562.

Kittrick, J.A., and Peryea, F.J. (1988) Experimental validation of the monophase structure model for montmorillonite stability. Soil Science Society of America Journal, 52, 199–201.

——— (1989) The monophase model for Mg-saturated montmorillonite. Soil Science Society of America Journal, 53, 292–295.

Köster, H.M. (1977) Die Berechnung kristallchemischer Strukturformeln von 2:1-Schichtsilikaten unter Berücksichtigung der gemessenen Zwischenschichtladungen und Kationenumtauschkapazitäten, sowie die Darstellung der Ladungsverteilung in der Struktur mittels Dreieckkoordinaten. Clay Minerals, 12, 45–54.

——— (1979) Die chemische Silikatanalyse, 196 p. Springer-Verlag, Berlin.

——— (1982) The crystal structure of 2:1 layer silicates. In Proceedings of the 7th International Clay Conference, Bologna, Pavia, Italy, 1981, 41–71.

Lagaly, G., and Weiss, A. (1969) Determination of the layer charge in mica-type layer silicates. Proceedings of the International Clay Conference, Tokyo, 1, 61–80.

Lippmann, F. (1982) The thermodynamic status of clay minerals. Proceedings of the International Clay Conference, Bologna and Pavia, Italy, 1981, 475–485.

Manceau, A. (1990) Distribution of cations among the octahedra of phyllosilicates: Insight from EXAFS. Canadian Mineralogist, 28, 321–328.

Manceau, A., Bonnin, D., Stone, W.E.E., and Sanz, J. (1990) Distribution of Fe in the octahedral sheet of trioctahedral micas by polarized EXAFS: Comparison with NMR results. Physics and Chemistry of Minerals, 17, 363–370.

Mason, R.A. (1992) Models of order and iron-fluorine avoidance in biotite. Canadian Mineralogist, 30, 343–354.

May, H.M., Kinniburg, D.G., Helmke, P.A., and Jackson, M.L. (1986) Aqueous dissolution, solubilities and thermodynamic stabilities of common aluminosilicate clay minerals: Kaolinite and smectites. Geochimica et Cosmochimica Acta, 50, 1667–1677.

McMurtry, G.M., Wang, C.H., and Yeh, H.W. (1983) Chemical and isotopic investigations into the origin of clay minerals from the Galapagos hydrothermal mounds field. Geochimica et Cosmochimica Acta, 47, 475–489.

Mehra, O.F., and Jackson, M.L. (1960) Iron oxide removal from soil and clays by a dithionite-citrate system buffered with bicarbonate. Clays and Clay Minerals, 7, 317–327.

Nadeau, P.H., Wilson, M.J., McHardy, W.J., and Tait, J.M. (1984) Interparticle diffraction: A new concept for interstratified clays. Clay Minerals, 19, 757–769.

Newman, A.C.D., and Brown, G. (1987) The chemical constitution of clays. Mineralogical Society Monograph, 6, 1–128.

Nickel, E.H., and Mandarino, J.A. (1987) Procedures involving the IMA Commission on New Minerals and Mineral Names, and guidelines on mineral nomenclature. Canadian Mineralogist, 25, 353–377.

Odin, G.S., and Matter, A. (1981) De glaconiarum origine. Sedimentology, 28, 611–641.

Ohr, M., Halliday, A.N., and Peacor, D.R. (1990) Sr and Nd isotopic evidence for punctuated clay diagenesis, Texas Gulf Coast. Earth and Planetary Science Letters, 105, 110–126.

Peacor, D.R. (1992a) Analytical electron microscopy: X-ray analysis. In Mineralogical Society of America Reviews in Mineralogy, 27, 113–140.

——— (1992b) Diagenesis and low-grade metamorphism of shales and slates. In Mineralogical Society of America Reviews in Mineralogy, 27, 335–380.

Petersen, N., von Dobeneck, T., and Vali, H. (1986) Fossil bacterial magnetite in deep-sea sediments from the South Atlantic Ocean. Nature, 320, 611–615.

Ransom, B., and Helgeson, H.C. (1989) On the correlation of expandability with mineralogy and layering in mixed-layer clays. Clays and Clay Minerals, 37, 189–191.

Rosenberg, P.E., Kittrick, J.A., and Aja, S.U. (1990) Mixed-layer illite/smectite: A multi-phase illite model. American Mineralogist, 75, 1182–1185.

Sheppard, R.A., Gude, A.J., and Griffin, J.J. (1970) Chemical composition and physical properties of phillipsite from the Pacific and Indian Oceans. American Mineralogist, 55, 2053–2062.

Singer, A., Stoffers, P., Heller-Kallai, L., and Szafranek, D. (1984) Nontronite in a deep-sea core from the South Pacific. Clays and Clay Minerals, 32, 375–383.

Stonecipher, S.A. (1978) Chemistry of deep-sea phillipsite, clinoptilolite, and host sediment. In L.B. Sand and F.A. Mumpton, Eds., Natural zeolites: Occurrence, properties, use, p. 221–234. Pergamon, Elmsford, New York.

Tardy, Y., and Duplay, J. (1992) A method of estimating the Gibbs free energies of formation of hydrated and dehydrated clay minerals. Geochimica et Cosmochimica Acta, 56, 3007–3029.

Vali, H., and Bachmann, L. (1988) Ultrastructure and flow behavior of colloidal smectite dispersions. Journal of Colloid and Interface Science, 126, 278–291.

Vali, H., and Hesse, R. (1990) Alkylammonium ion treatment of clay minerals in ultrathin sections: A new method for HRTEM examination of expandable layers. American Mineralogist, 75, 1445–1448.

——— (1992a) The microstructure of dilute clay and humic acid suspensions revealed by freeze-fracture electron microscopy: Discussion. Clays and Clay Minerals, 40, 620–623.

——— (1992b) Identification of vermiculite by transmission electron microscopy (TEM) and X-ray diffraction. Clay Minerals, 27, 185–192.

Vali, H., and Kirschvink, J. (1989) Magnetofossil dissolution in a palaeomagnetically unstable deep sea sediment. Nature, 339, 2203–2206.

Vali, H., and Köster, H.M. (1986) Expanding behaviour, structural disorder, regular and random irregular interstratification of 2:1 layer-silicates studied by high-resolution images of transmission electron microscopy. Clay Minerals, 21, 827–859.

Vali, H., Förster, O., Amarantidis, G., and Petersen, N. (1987) Magnetotactic bacteria and their magnetofossils in sediments. Earth and Planetary Science Letters, 86, 389–400.

Vali, H., von Dobeneck, T., Amarantidis, G., Förster, O., Morteani, G., Bachmann, L., and Petersen, N. (1989) Biogenic and lithogenic magnetic minerals in Atlantic and Pacific deep sea sediments and their paleomagnetic significance. Geologische Rundschau, 78/3, 753–764.

Vali, H., Hesse, R., and Kohler, E.E. (1991) Combined freeze-etch replicas and HRTEM images as tools to study fundamental-particles and the multi-phase nature of 2:1 layer silicates. American Mineralogist, 76, 1973–1984.

Vali, H., Hesse, R., and Kodama, H. (1992) Arrangement of *n*-alkylammonium ions in phlogopite and vermiculite: An XRD- and TEM-study. Clays and Clay Minerals, 40, 240–245.

Velde, B. (1985) Clay minerals: A physico-chemical explanation of their occurrence. Developments in Sedimentology, 40, 428 p.

Velde, B., and Brusewitz, A.M. (1986) Compositional variation in component layers in natural illite/smectite. Clays and Clay Minerals, 34, 651–657.

Velde, B., and Meunier, A. (1987) Petrologic phase equilibria in natural clay systems. In Mineralogical Society, Monograph, 6, 423–458.

Warren, E.A., and Ransom, B. (1992) The influence of analytical error upon the interpretation of chemical variations in clay minerals. Clay Minerals, 27, 193–209.

Zierold, K. (1987) Cryoultramicrotomy. In R.A. Steinbrecht and K. Zierold, Eds., Cryotechniques in biological electron microscopy, p. 132–148. Springer-Verlag, Berlin.

Manuscript received December 23, 1992
Manuscript accepted August 1, 1993